Journal of New Materials for Electrochemical Systems 13, 119-126 (2010)

Electrodeposition of Silver Particles on an ITO Substrate in Room Temperature Ionic Liquids (RTILs) of 1-Ethyl-3-Methylimidazolium Tetrafluoroborate ($EMIBF_4$)

Qingfei Wang, Zhenman Sun and Keqiang Ding*

College of Chemistry and Materials Science, Hebei Normal University, Shijiazhuang, 050016, P.R. China

Received: May 19, 2009, Accepted: January 25, 2010

Abstract: *In room temperature ionic liquids (RTILs) of 1-ethyl-3-methylimidazolium tetrafluoroborate ($EMIBF_4$), for the first time, silver (Ag) particles were successfully electrodeposited onto an indium tin oxide (ITO)-coated glass substrate by galvanostat and cyclic voltammetry (CV) methods, respectively. The obtained scanning electron microscopy (SEM) images not only demonstrated that silver particles were fabricated on the ITO substrate, but also indicated that the applied current density is the main factor affecting the morphologies of silver particles prepared by the galvanostat method. Subsequently, the obtained cyclic voltammograms (CVs) indicated that the electrodeposition mechanism of Ag particles on the ITO substrate is different from that on the Ag-coated ITO substrate, as was also discussed by chronoamperometry based on the previously developed nucleation mode. Presenting the generation of sliver particles onto an ITO substrate in RTILs is the main contribution of this paper.*

Keywords: Silver particles; RTILs; Galvanostat method; Cyclic Voltammetry (CV); Chronoamperometry; Nucleation.

1. INTRODUCTION

Due to the key applications of metal nanoparticles in electrocatalysis, many methods were developed to prepare metal nanoparticles [1, 2]. Recently, silver nanoparticles have attracted considerable interest because of its application in electrocatalysis and oxygen reduction reaction (ORR). For example, Lin [3] prepared colloidal silver nanoparticles-modified electrode and studied its electrocatalysis towards the electrochemical behavior of Cytochrome *c*, in which silver nanoparticles were prepared by the reduction of $AgNO_3$ using $NaBH_4$ as reducing agents. Shao [4] prepared silver-modified $Ba_{0.5}Sr_{0.5}Co_{0.8}Fe_{0.2}O_{3-\delta}$ (BSCF) cathodes used in the intermediate-temperature solid-oxide fuel cells, on which ORR was thoroughly investigated. Generally, there are two typical methods to fabricate metal particles, i.e., (a) chemical reduction, as addressed in ref. [3] and [4]. (b) electrochemical method, for instance, Yang [5] electrodeposited silver nanoparticles onto an mercaptoacetic acid coated gold electrode by potentiodynamic and potentiostatic techniques, in which the obtained silver nanoparticles were characterized by SEM.

Room temperature ionic liquids (RTILs) have received considerable attention due to its excellent features, for instance, low-volatility, non-toxicity, non-flame, higher conductivity compared to the common organic solvent, and higher solubility for organic substance when comparing with the aqueous solution [6-9]. Unfortunately, to the best of our knowledge, the application of RTILs in large scale was poorly reported, i.e., the significant application of RTILs still remains unrevealed though numerous papers concerning RTILs were published every year. Thus, developing novel applications of RTILs has become into an important task for chemistry researchers. We have successfully utilized RTILs as electrolytes in probing ORR [10], bioelectrochemistry fields [11] and preparation of polymers [12]. The electrodeposition of silver particles in RTILs has been reported by A. M. Bond [13], in which silver nanoparticles were prepared onto a glassy carbon electrode from a kind of RTILs of DIMCARB [14] by electrochemical methods.

ITO (Indium Tin Oxides) is a highly degenerated n-type semiconductor, with a low electrical resistivity of 2×10^{-4} Ω• cm and a wide band gap (from 3.3 eV to 4.3 eV) [15], showing a high transmission in the visible range. ITO-coated glass has been widely used as a substrate in many applications including solar cells, heat-reflecting mirrors, antireflective coatings, gas sensors and flat panel displays [16]. For instance, Ballarin [17] fabricated self-

*To whom correspondence should be addressed: Email: dkeqiang@263.net

assembled gold nanoparticles modified ITO electrodes, in which ITO glass was functionalized by bifunctional crosslinkers prior to the self-assembly process. Dong [18] prepared poly(aniline-co-o-aminobenzenesulfonic acid) three-dimensional tubal net-works modified ITO electrode and studied its catalysis towards the electrochemical behavior of Cytochrome *c*. ITO glass was also utilized in our previous work, in which a MnO_2-coated ITO electrode was prepared by a CV technique[19]. Thus, it can be concluded that ITO glass is an ideal substrate on which electrochemical experiment could be performed very well. Summarily, based on the previous literatures, to our knowledge, so far, there is no paper reporting the electrodeposition of silver particles onto an ITO substrate in RTILs of $EMIBF_4$.

In this paper, silver particles were electrodeposited onto an ITO substrate from RTILs of $EMIBF_4$ by a galvanostat method, followed by the characterization of SEM images. Then, CV technique was employed to fabricate the silver particles-modified ITO substrate, and it was found that CVs obtained on the ITO substrate were different from that obtained on the silver-coated ITO substrate. Lastly, the nucleation mechanism of silver particles on the ITO substrate and on the Ag-coated ITO substrate was preliminarily probed by chronoamperometry. Presenting the fact that Ag particles could be electrodeposited onto an ITO substrate from RTILs of $EMIBF_4$ is the main contribution of this paper.

2. EXPERIMENTAL

2.1. Chemicals and materials

Room temperature ionic liquids (RTILs) of 1-ethyl-3-methylimidazolium tetrafluoroborate ($EMIBF_4$) with a purity of more than 99% were bought from Hangzhou Chemer Chemical CO., Ltd (China). ITO (Indium Tin oxides) glass substrates were purchased from Shenzhen Hivac Vacuum Photo-Electronics Co. Ltd (China).The molecular structure of $EMIBF_4$ is shown in scheme 1. Silver nitrate and other used reagents were all purchased from Tianjin Chemical Reagent Co. Ltd (China).

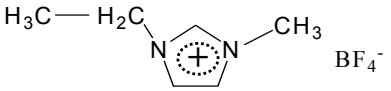

Scheme 1. $EMIBF_4$

2.2. Apparatus

Scanning electron microscopy (SEM) was performed on a Hitachi S-570 microscope (Japan) operated at 20kV. Electron diffraction spectroscopy (EDS) was recorded on a WD-8 X-ray energy instrument (Japan). Electrochemical measurements were all conducted on a CHI 660B electrochemical workstation (Shanghai Chenhua Apparatus, China).

2.3. Preparation of silver particles onto an ITO substrate

In the electrochemical measurement, a conventional three-electrode cell was employed, in which an ITO glass (geometrical area is 0.4 cm^2) was used as the working electrode, and a platinum wire and a quasi Ag electrode were utilized as the counter and reference electrode, respectively. It should be mentioned that the quasi-reference electrode was prepared according to the previous literature [20], i.e., a well-cleaned silver wire was immersed into $EMIBF_4$ solution containing 1mM Ag^+ (in form of $AgNO_3$), giving rise to a quasi reference electrode (denoted as Ag^+/Ag), and the quasi reference electrode was separated from the bulk solution with a glass frit while using.

Prior to the experiment, the ITO substrate was dipped into acetone at least for 5 min to remove the adsorbed greases, and then the ITO substrate was thoroughly rinsed by redistilled water. Before dipping into the RTILs of $EMIBF_4$, the as-cleaned ITO substrate must be dried by air to avoid introducing water into $EMIBF_4$ solution. The auxiliary electrode of platinum wire was immersed in a concentrated nitric acid for 2 min, and then the auxiliary electrode was rinsed by the doubly distilled water thoroughly and dried by air. To avoid the influence of oxygen, prior to experiment, nitrogen gas was bubbled into $EMIBF_4$ at least for 20 min to remove the dissolved oxygen molecules. It must be noted that during the experiment, nitrogen gas was flowed over the RTILs of $EMIBF_4$ to avoid the interference of oxygen and water.

3. RESULTS AND DISCUSSION

3.1. SEM images for the silver particles obtained by galvanostat method

Galvanostat method is a method in which the current between the working electrode and counter electrode was kept constant. For the electrochemical reduction reaction, a cathode current should be applied through the potentiostat/galvanostat instrument. Galvanostat method has been widely employed to fabricate metal particles mainly due to its simple manipulation [21]. In this work, various cathodic currents were applied onto the well-cleaned ITO substrate, and the applied period was 5 min. The obtained samples are shown in Fig.1. As can be seen, when the current density is 15μA/cm^2, several large flower-like particles are exhibited as shown in image A of Fig.1, while as the current density is 25μA/cm^2, except for the flower-like particles, some smaller particles were formed on the ITO substrate, as shown by image B. With the increasing of current density, more small particles were generated on the ITO substrate as shown by image C and image D. Tafel plot tells one that the lower current density leads a lower overpotential, and higher current generates a higher overpotential [22]. As reported previously [23], the lower overpotential favors the two-dimensional (2D) nucleation and growth, and the higher overpotential benefits the three-dimensional (3D) growth controlled by the incorporation of adatoms into the lattice. That is to say, lower overpotential is favorable to the nucleation and crystallization growth over the substrate surface, thus, as the current densities were lower, some larger particles were exhibited as shown in image A of Fig.1. While as the current densities were higher, three-dimensional (3D) growth was favored, giving rise to small particles. Additionally, as demonstrated in previous studies [24] of metal deposition on single-crystal substrate, surface defects provide nucleation sites of a different nature to the rest of the homogeneous surface, and the deposition process was facilitated at these defects. Probably, when the overpotential is higher, more potential defects on the ITO substrate were activated, giving rise to more surface defects on which nucleation and crystallization process could proceed easily, leading to the generation of more small particles as shown by image C and D.

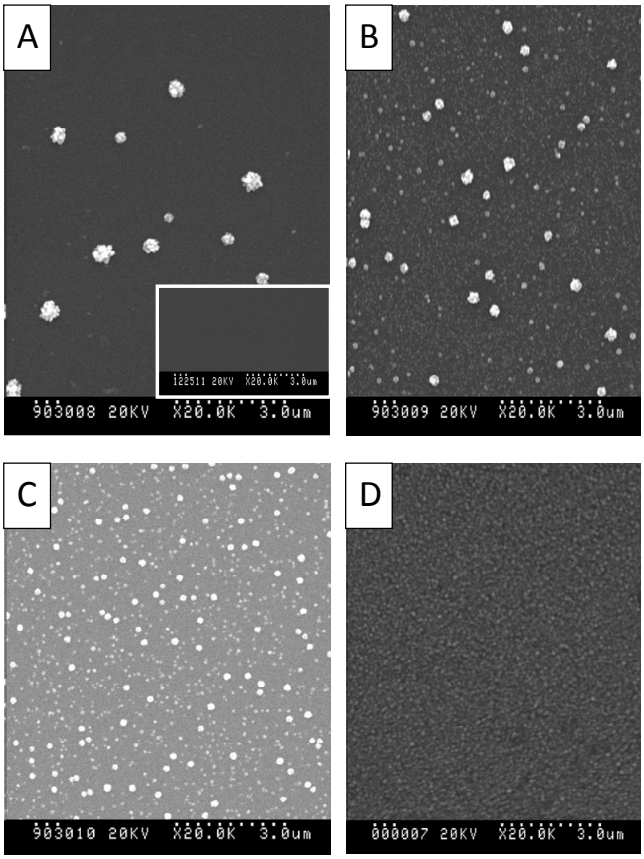

Figure 1. SEM images of Ag particles prepared from EMIBF4 having 5mM Ag^+ by galvanostat method, in which the perturbation is 5 min and the applied constant current densities are different. (A): 15μA/cm^2 (B): 25μA/cm^2 (C): 50μA/cm^2 (D):100μA/cm^2. The inset image in image A is the pure ITO substrate employed.

To confirm the existence of silver elements, EDS spectra was measured as shown in Fig.2, in which the absorption peak of silver was clearly exhibited. It should be mentioned that before SEM measurement, to get clear images, Au vapor was sprayed on the samples, thus, the peak corresponding to Au was displayed in the EDS spectra. Evidently, element of Si exhibited in EDS spectra was resulted from the glass used.

3.2. Cyclic Voltammograms (CVs) of Ag^+ in $EMIBF_4$

Cyclic voltammetry (CV) has been used as a powerful technique to fabricate nanoparticles mainly owing to its simple manipulation. For example, Fang [25] prepared platinum nanoparticles onto aligned carbon nanotubes (ACNTs) from an aqueous solution of H_2PtCl_6 by CV successfully. As described in ref.5, silver nanoparticles was also prepared by CV.

Fig.3 is the typical cyclic voltammograms (CVs) for $EMIBF_4$ containing 0.5mM Ag^+, which was obtained at 50mV/s for 10 cycles. The dotted line in Fig.3 is the CVs obtained in $EMIBF_4$, suggesting that ITO-coated glass substrate is electrochemically stable, or in other words, no electrochemical reaction of ITO was found during potential sweep, allowing us to use ITO glass as a substrate.

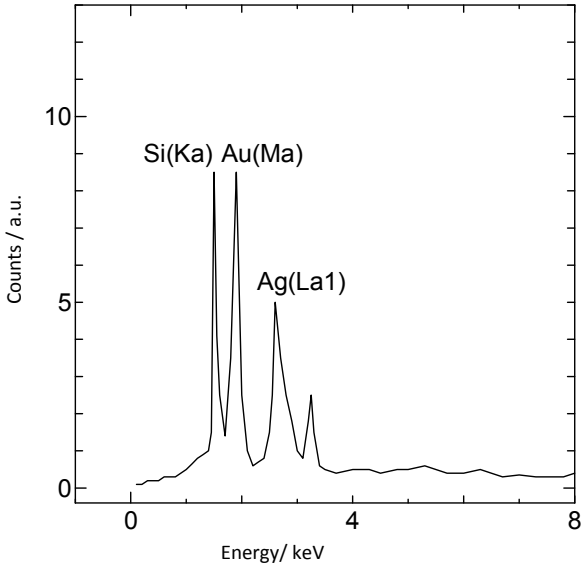

Figure 2. EDS spectra of the obtained Ag particles.

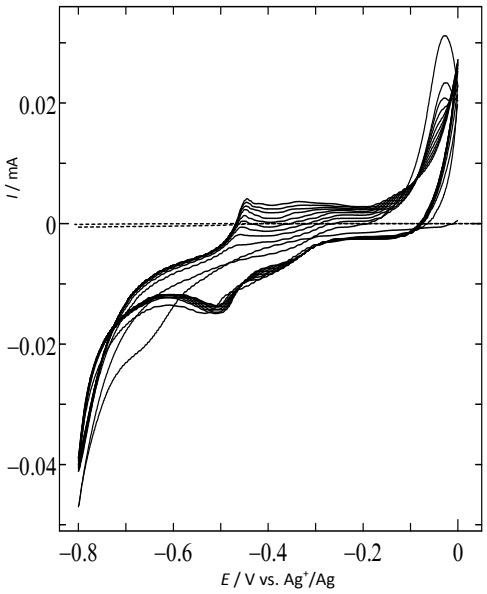

Figure 3. Cyclic Voltammograms (CVs) obtained on an ITO electrode in EMIBF4 containing 0.5 mM Ag^+, in which the dotted line was obtained in the absence of Ag^+. CVs were recorded at 50mV/s for 10cycles.

When silver ions (in form of $AgNO_3$) were introduced, several couples of redox peaks are observed in the employed potential range. Here, it can be seen that with the increasing of sweep cycle numbers, peak current gradually enhanced, suggesting that some substances were formed on the ITO substrate based on our previous work[26]. After scrutinizing Fig.3, as can be seen, with the increasing of cycle numbers, the reduction peak current at around -0.5V enhanced obviously, however, its oxidation peak was not clearly

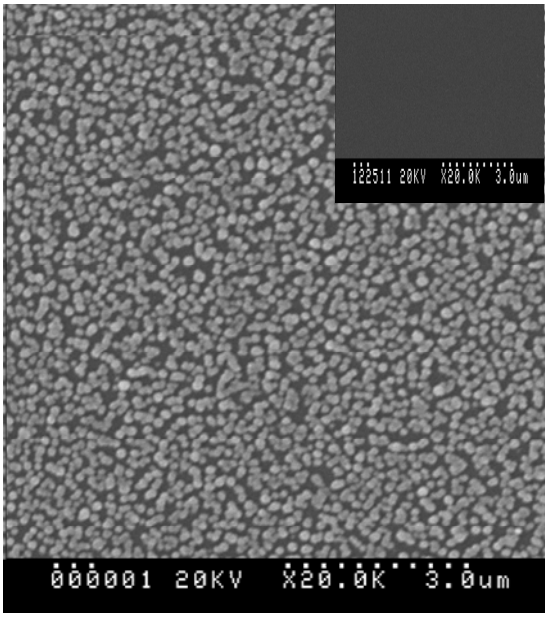

Figure 4. SEM images of Ag particles prepared by CV as shown in Fig.3. The inset in the top right corner is the pure ITO substrate used.

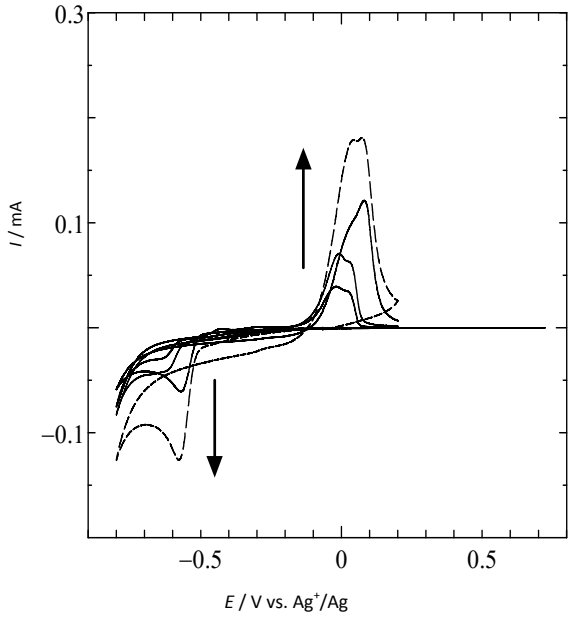

Figure 5. CVs obtained in EMIBF4 containing various concentrations of Ag^+ on an ITO electrode; the concentrations of Ag^+ are 0.5, 1, 2, 5mM, respectively. Scan rate: 50mV/s.

exhibited though there are some oxidation current plateaus displayed in the potential range from -0.44V to -0.2V. Generally, a current plateau in CVs corresponds to an ideal capacitance behavior, thus, this capacitance behavior supported that some substances were formed on the ITO substrate because of the continuous potential sweep. The peak at -0.8V and that at around 0 V will be discussed as follows. Fig.4 is the SEM images obtained by CV as described in Fig.3, strongly indicating that CV is a feasible technique to electrodeposite Ag particles onto the ITO substrate. Compared to those particles generated by the galvanostat method, it seems that the particles prepared by CV are more uniform. To our knowledge, this is the first time to report the immobilization of Ag particles by CV on an ITO substrate.

To confirm the origin of peaks observed in Fig.3, CVs of Ag^+ with various concentrations are displayed in Fig.5. One can see that with the increasing of concentration, both the reduction peak at about -0.5V and oxidation peak at 0 V all enhanced evidently. For instance, the dashed line in Fig.5 is the CVs for 5mM Ag^+ in $EMIBF_4$, whose peak currents, including the reduction peak current and oxidation peak current, are the largest ones among these peaks exhibited. Therefore, it is reasonable to attribute the reduction peak at -0.5V to the electrochemical reduction of Ag^+. Meanwhile, the reduction peak at -0.5V is a normal peak, i.e., a hill-like peak, indicating that the electrochemical reduction process of Ag^+ was controlled by a diffusion process (as was proved by the linear relationship between peak current and square root of scan rate, which was not presented in this paper). Interestingly, the oxidation peak is an abnormal peak with irregular shape. In principle, the peak potential separation of ΔE_p, i.e., $\Delta E_p=E_{pa}-E_{pc}$ (E_{pa} and E_{pc} are the anodic peak potential and the cathodic peak potential, respectively.), should be close to 59 mV if the reversible electrochemical process contains one electron [27]. As for Fig.5, the value of ΔE_p alters greatly when the concentration of Ag^+ was different. Besides, cursory estimation tells one that the charge consumed by the reduction of Ag^+ does not amount to the charge consumed by its oxidation process, if we supposed that the peak area is reckoned as the charge consumed. Hence, the oxidation peak at 0V should not correspond to the electrochemical oxidation of Ag, though Palomar-Pardavé [28] has thought that the oxidation peak at 0.04V vs SCE corresponds to the silver dissolution from a vitreous carbon substrate. Probably, the oxidation peak appearing at 0V corresponds to a mixed process that contains the dissolution of Ag from ITO substrate to $EMIBF_4$ and other unknown processes. More direct proofs are really required in the further work.

Additionally, with the increase of Ag^+ concentration, the reduction peak was dramatically positively shifted, implying that the higher concentration of Ag^+ lowered the overpotential of the electrochemical reduction of Ag^+, as seldom observed in the aqueous solution. Probably, along with the formation Ag particles on the ITO substrate, the electrochemical reduction process of Ag^+ was accelerated, that is to say, the reduction mechanism of Ag^+ on the ITO substrate should be different from that on the Ag-coated ITO substrate. Interestingly, in contrast to the reduction peak, the oxidation peak potential was slightly positively shifted when the concentration of Ag^+ was increased, implying that the oxidation reaction of Ag became more difficult as the concentration of Ag^+ was increased. Maybe, due to the formation of silver particles on the ITO substrate, the overpotential of electrochemical oxidation of Ag was enhanced correspondingly, leading to a positive-shifting of oxidation peak potential. Unfortunately, due to the limited solubility of $AgNO_3$ in $EMIBF_4$, CVs for the higher concentrations of Ag^+ were not measured.

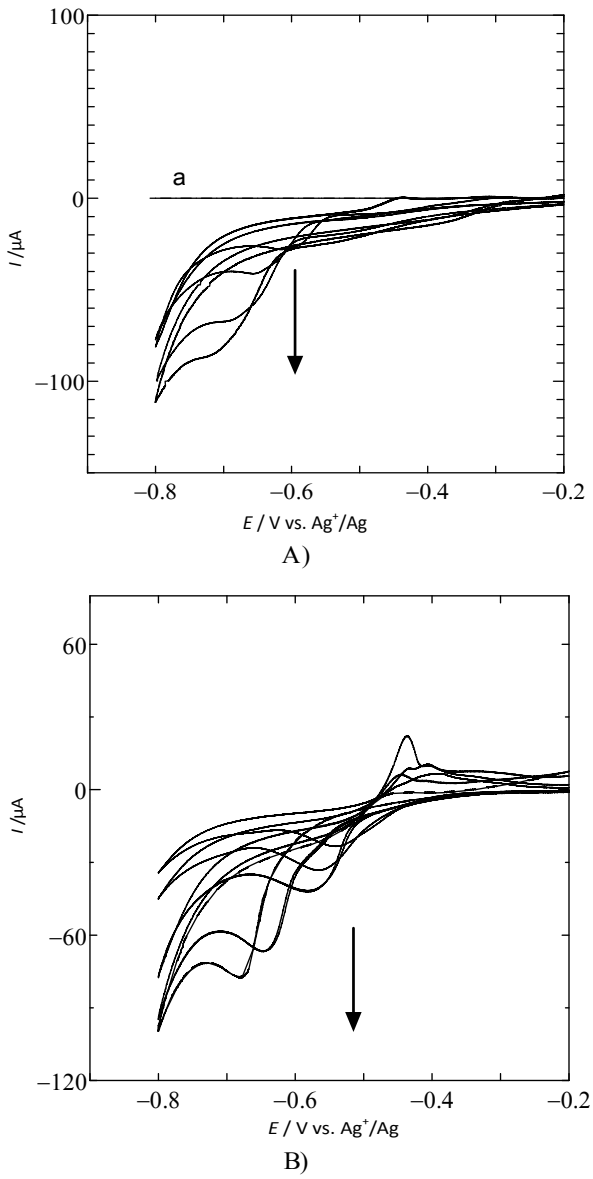

Figure 6. A) CVs obtained on an ITO electrode in EMIBF4 containing 0.5 mM Ag^+, in which line **a** was obtained in the absence of Ag^+. The scan rates are 10, 20, 50, 100, 150 mV/s, respectively. B) CVs obtained on the Ag-coated ITO electrode in $EMIBF_4$ containing 0.5 mM Ag^+, the scan rates are 10, 20, 50,100,150, 300mV/s, respectively.

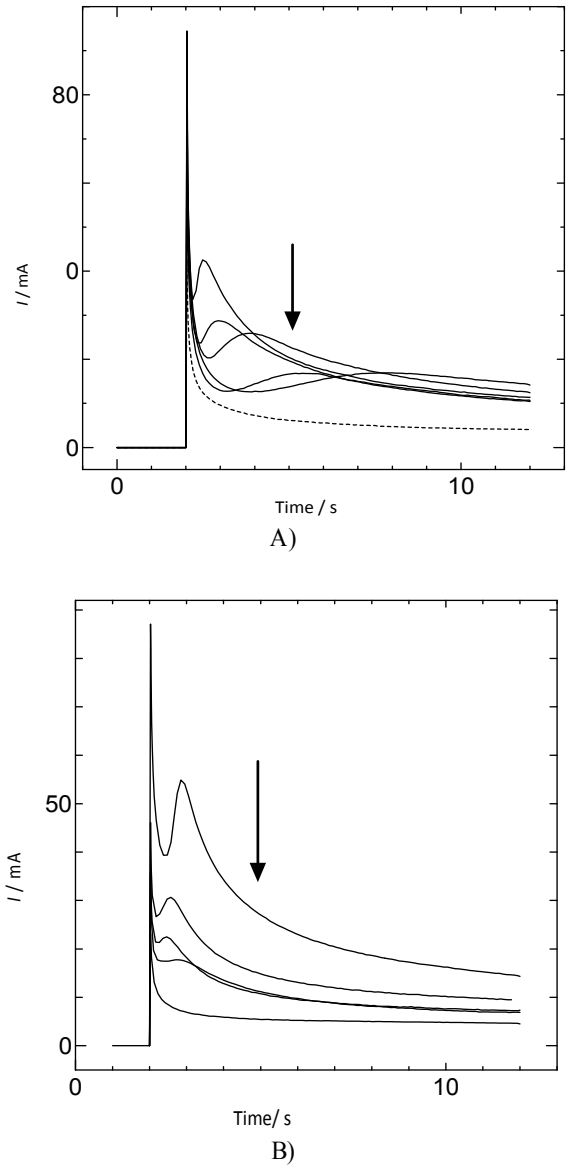

Figure 7. A) I-t curves obtained by applying various potentials on the ITO substrate. From up to down the applied potentials are -0.61, -0.59,-0.57,-0.55,-0.53 and -0.48V vs Ag^+/Ag reference electrode. B) I-t curves obtained by applying various potentials on the Ag-coated ITO substrate. From up to down the applied potentials are -0.59, -0.57, -0.55,-0.53 and -0.51V vs Ag^+/Ag reference electrode.

As documented above, it seems that the reduction mechanism of Ag^+ on the ITO substrate differs from that on the Ag-coated ITO, therefore, the influence of scan rate on the reduction peak of Ag^+ was performed on the ITO substrate and Ag-coated ITO substrate, respectively, as shown in Fig.6A and Fig.6B. Here, the Ag-coated ITO is the ITO substrate on which Ag particles were electrodeposited by CV for 10 cycles as illustrated in Fig.3. It can be seen that as shown in Fig.6A,with the increase of scan rate, the reduction peak current enhanced correspondingly, a well-defined line describing the relationship between the reduction peak current and the square root of scan rate was obtained (data not shown here), suggesting that the reduction reaction of Ag^+ on the ITO substrate was controlled by a diffusion-process, meanwhile, one can observe that with the increase of scan rate, the reduction peak potential was slightly negatively shifted. While for the case on the Ag-coated ITO substrate, as shown in Fig.6B, the reduction peak potential was dramatically negatively shifted when the scan rate was increased, indicating that when the scan rate is high, the overpotential corresponding to the reduction reaction of Ag^+ was enhanced greatly. The comparison between Fig.6A and Fig.6B intrigued us to probe

the nucleation process of those silver particles immobilized on different substrates, as shown below.

3.3. Chronoamperometry

To clarify the nucleation mechanism of Ag particles, chronoamperometry [23] was employed. The obtained i-t curves are shown in Fig.7A and Fig.7B. Fig.7A was obtained by applying the various potentials on the ITO substrate for 12s, in which the applied potential from up to down were -0.61, -0.59,-0.57,-0.55,-0.53 and -0.48V, respectively. One can see that when the applied potential is -0.61V, there is a current peak appearing at around 3s, and then the current value was dramatically attenuated. When the applied potential is -0.48V, as shown by the dotted line in Fig.7A, no current peak was observed, suggesting that no reduction reaction of Ag^+ took place. It also can be seen that the current peak was varied from a sharper peak to a sluggish one as the applied potential ranged from -0.61V to -0.48V. Additionally, the peak-time(t_m), corresponding to the current peak, was also increased with the variation of applied potentials when ranging from -0.61V to -0.48V. The shape of Fig.7A is very similar to the published [29] plots describing the simulated transient for instantaneous nucleation. Fig.7B was obtained by applying the various potentials on the Ag-coated ITO substrate, in which the applied potentials from up to down were -0.59, -0.57,-0.55,-0.53 and -0.51V, respectively. As shown in Fig. 7B, also, there a current peak at a certain time in each curve. Interestingly, the peak-times are almost identical, which is significantly different from that exhibited in Fig 7A. We also notice that, in Fig.7A, the values of steady-state current plateau appearing in i-t curves almost remain constant except for the case when the applied potential is -0.48V. However, the steady-state current plateau in Fig.7B was evidently lowered when the applied potential was changed from -0.59V to -0.51V. Generally, the steady-state current plateau corresponds to a capacitance-like electrode [30], which can reflect the variation of the modifiers on the electrode surface, or in other words, as the substances immobilized on the electrode are different, various steady-state current plateaus should be exhibited. Thus, based on the various current peaks and current plateaus, one can conclude that the reduction process of Ag^+ on the ITO substrate differs from that on the Ag-coated ITO substrate.

Based on the previous reports [31], so far, there are two typical nucleation modes proposed. One was the instantaneous nucleation mode that metal atoms were deposited at the same time in the infinite active sites on the electrode surface, the other one was the progressive nucleation mode that the metal atoms were deposited in the finite active sites on the electrode surface one by one. Correspondingly, there are two formulas describing above nucleation modes when using chronoamperometry to probe the nucleation mode [32], as shown below.

$$\left(\frac{I}{I_m}\right)^2 = \frac{1.9542}{(t/t_m)}\left\{1-\exp\left[-1.2564\left(\frac{t}{t_m}\right)\right]\right\}^2 \quad (1)\ \text{instantaneous nucleation}$$

$$\left(\frac{I}{I_m}\right)^2 = \frac{1.2254}{(t/t_m)}\left\{1-\exp\left[-2.3367\left(\frac{t}{t_m}\right)^2\right]\right\}^2 \quad (2)\ \text{progressive nucleation}$$

In which, I was current at time t and I_m was the maximum current obtained at time t_m.

By plotting the experimentally obtained (I/I_m) vs. (t/t_m) [13] and overlaying the values for the theoretical curves, a direct comparison can be made. The data used in Fig.8A was selected from the first curve of Fig.7A measured at -0.61V. The thick solid line is the

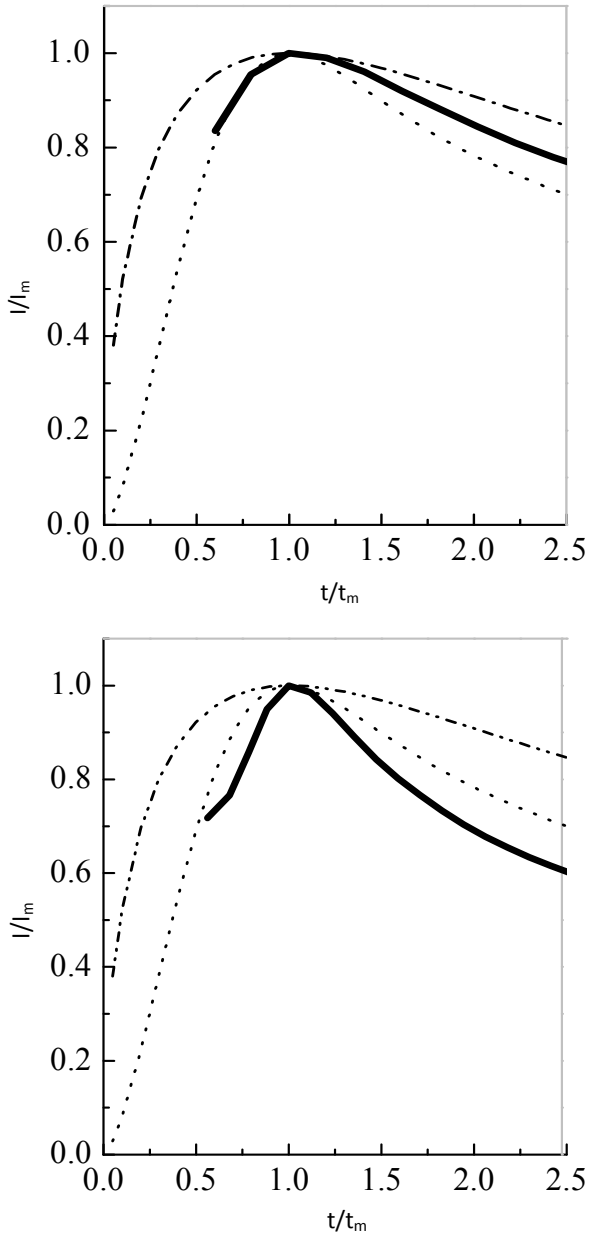

Figure 8. A) Curves of dimensionless current against time, in which the datum were selected from the curve at -0.61V in Fig.7A. The dot-dashed line represents the instantaneous nucleation model and the dotted line corresponds to a progressive nucleation model, the thick solid line was plotted based on the measured data.
B) Curves of dimensionless current against time, in which the datum were selected from the curve at -0.59V in Fig.7B. The dot-dashed line represents the instantaneous nucleation model and the dotted line corresponds to a progressive nucleation mode, the thick solid was curved based on the experimentally obtained data.

experimentally obtained plot, while the dot-dashed line and dotted line were obtained based on the formula (1) and formula (2), respectively. It can be seen that at the initial stage, the thick solid line fits the progressive nucleation plot very well, however, as the value of t/t_m exceeds unit, the deviation between the real line and theoretical line gradually increased. Similar results were obtained when other potentials, i.e., -0.59,-0.57,-0.55,-0.53 V, were employed. These results strongly demonstrated that at the initial stage, the electrodeposition of silver particles was mainly dominated by a progressive nucleation process. Probably, the progressive nucleation model could partially account for the formation of silver particles with large size as shown in Image A of Fig.1. The data used in Fig.8B was chosen from the curve of Fig.7B plotted at -0.59 V, in which the thick solid line was plotted based on the experimentally obtained data, and the dot-dashed line and dotted line were curved based on the formula (1) and formula (2), respectively. Obviously, the obtained plot could not fit the theoretical line, though the tendency of thick solid line is similar to that of the dotted line in some degree. Thus, based on the plots in Fig.8A and Fig.8B, it can be inferred that the nucleation process on the ITO substrate accords with the progressive nucleation mode to some extent, and the nucleation process on the Ag-coated substrate is a complex nucleation mode. Therefore, on the ITO substrate, the progressive nucleation model generated a silver-immobilized ITO surface that has uniform structure, leading to a slightly negative shifting of reduction peak potential when the scan rate was increased as shown in Fig.6A. While on the Ag-coated ITO substrate, the complex nucleation model yielded a complex surface coated by silver particles, giving rise to a dramatically negative shifting of reduction peak potential when the scan rates were enhanced, as shown in Fig.6B.

We must admit that the preparation of silver particles by electrochemical method was a complex process [28], which is related to many factors, such as potential, electrolyte, current densities, and etc. Also due to our limited techniques, the exact formation mechanism of silver particles on ITO substrate in $EMIBF_4$ could not be well revealed in this preliminary work, and more works are required in the further investigation. But, we are confident that this is the first time to report the immobilization of silver particles onto ITO substrates by both galvanostat method and CV in RTILs of $EMIBF_4$, as is the main contribution of this work.

4. CONCLUSION

In this paper, silver particles were successfully electrodeposited onto an ITO substrate from RTILs of $EMIBF_4$ containing Ag^+ by galvanostat method and CV, respectively. SEM images of silver particles indicated that the morphologies of Ag particles are related to the applied constant current densities closely, and it was revealed that the lower current density is favorable to the formation of larger particles and the higher current density is beneficial to the generation of small particles with uniform distribution. Also, it was demonstrated that CVs of Ag^+ obtained on the ITO substrate are different from that obtained on the Ag-coated ITO substrate. Using Chronoamperometry technique, the possible nucleation process of Ag particles was discussed based on the previously developed formula, testifying that the nucleation process of Ag particles on the ITO substrate suits the progressive nucleation mode in some degree, and that on the Ag-coated substrate was thought as a complex one. Further works are in progress.

5. ACKNOWLEDGEMENTS

This work was financially supported by the Doctor Fund of Hebei Normal University, Key Project of Hebei Province Education Bureau (ZH2007106), Key Project Fund of Hebei Normal University (L2008Z08) and Special Assist Project of Hebei Province Personnel Bureau(106115).

REFERENCES

[1] Y. Li, Y. Wu, B. S. Ong, J. Am. Chem. Soc., 127, 3266 (2005).
[2] C. R. De Silva, S. Smith, I. Shim, J. Pyun, T. Gutu, J. Jiao, Z. Zheng, J. Am. Chem. Soc., DOI: 10.1021/ja9014277.
[3] L. Lin , P. Qiu , X. Cao , L. Jin, Electrochim. Acta, 53, 5368 (2008).
[4] W. Zhou,R. Ran , Z. Shao, R. Cai , W. Jin, N. Xu , J. Ahn, Electrochim. Acta, 53, 4370 (2008).
[5] N. Yang, X. Wang, Q. Wan, Electrochim. Acta, 52, 4818 (2007).
[6] T. Welton, Chem. Rev., 99, 2071 (1999).
[7] R. M. Lau, F. Rantwijl, K. R. Seddon, R. A. Sheldon, Org. Lett., 2, 4189 (2000).
[8] M. P.Jensen, Dzielawa, J. A.; Rickret, P.; Dietz, M. L.; J. Am. Chem. Soc., 124, 10664 (2002).
[9] J. S. Lee, N. D. Quan, J. M. Hwang, J.Y. Bae, H. Kim, B. W. Cho, H.S. Kim, H. Lee, Electrochem. Commun., 8, 460 (2006).
[10]K.-Q. Ding, T. Okajima, T. Ohsaka, Electrochemistry,75, 35 (2007).
[11]K.-Q., Ding, J. Chin. Chem. Soc., 54, 1179 (2007).
[12]K.-Q, Ding, Bull. Electrochem., 23, 193 (2007).
[13]A. I. Bhatt, A. M. Bond, J. Electroanal. Chem., 619–620, 1(2008).
[14]J. Zhang, A.I. Bhatt, A.M. Bond, A.G. Wedd, J. L. Scott, C.R. Strauss, Electrochem. Commun., 7, 1283(2005).
[15]K. Kim, N. Man, T. Kim, K. S. Cho, H. Y. Chu, J. Lee, G. Y. Sung, ETRI J., 27, 405(2005).
[16]H. Kim, Howitz, J. S.; Kushto, G.; Pique, A. ; Kafafi, Z. H.; Gilmore, C. M.; Chrisey, D. B. J. Appl. Phys., 88, 6021 (2000).
[17]B. Ballarin, M. C. Cassani, E. Scavetta, D. Tonelli, Electrochim. Acta, 53, 8034 (2008).
[18]X. Jiang, L. Zhang, S. Dong, Electrochem. Commun., 8, 1137 (2006).
[19]K.-Q, Ding, J. Chin. Chem. Soc., 56, 175 (2009).
[20]G. A. Snook , A. S. Best, A. G. Pandolfo, A. F. Hollenkamp, Electrochem. Commun., 8, 1405 (2006).
[21]L. Huang, H.-B. Wei , F.-S. Ke , X.-Y. Fan, J.-T. Li , S.-G. Sun, Electrochim. Acta, 54, 2693 (2009).
[22]M.-Y. Shen, S.-P. Chiao, D.-S. Tsai, D. P. Wilkinson, J.-C. Jiang, Electrochim. Acta, 54, 4297 (2009).
[23]M. Palomar-Pardavé, M. Miranda-Hernández, I. González, N. Batina, Surf. Sci., 399, 80 (1998).
[24]W. J. Lorenz, G. Staikov, Surf. Sci., 335, 32 (1995).
[25]J. Yang, R. Zhang, Y. Xu, P. He, Y. Fang, Electrochem. Commun., 10, 1889 (2008).
[26]K.-Q. Ding, J. Chin. Chem. Soc., 55, 543 (2008).

[27]K.-Q, Ding, F. Wang, M. Zhao. J. Chin. Chem. Soc., 54, 723 (2007).
[28]M. Palomar-Pardavé, M. T. Ramírez, I. González, A. Serruya, B. Scharifker, J. Electrochem. Soc., 143, 1539 (1996).
[29]A. N. Correia, S. A. S. Machado, J. C. V. Sampaio, L. A. Avaca, J. Electroanal. Chem., 407, 37 (1996).
[30]J. N. Broughton, M. J. Brett, Electrochim. Acta, 50, 4814 (2005).
[31]B. R. Scharifker, J. Mostany, M. Palomar-Pardave, I. Gonzales, J. Electrochem. Soc., 146, 1005 (1999).
[32]C. Bjelkevig, J. Kelber, Electrochim. Acta, 54, 3892 (2009).